Quaternary Research 72 (2009) 337–346

Contents lists available at ScienceDirect

Quaternary Research

journal homepage: www.elsevier.com/locate/yqres

Spatial patterns of Holocene glacier advance and retreat in Central Asia

Summer Rupper [a,*], Gerard Roe [b], Alan Gillespie [b]

[a] Brigham Young University, Department of Geological Sciences, S389 ESC, Provo, UT 84602, USA
[b] University of Washington, Department of Earth and Space Sciences and Quaternary Research Center, Seattle, WA, USA

ARTICLE INFO

Article history:
Received 28 February 2008
Available online 8 August 2009

Keywords:
Climate
Paleoclimate
Glaciers
Energy balance
Monsoon
Asia
Holocene
Numerical model

ABSTRACT

Glaciers in the southern Himalayas advanced in the early Holocene despite an increase in incoming summer solar insolation at the top of the atmosphere. These glacier advances are in contrast to the smaller alpine glaciers in the western and northern regions of Central Asia. Two different glacier mass-balance models are used to reconcile this Holocene glacier history with climate by quantifying the change in equilibrium-line altitudes (ELA) for simulated changes in Holocene climate. Both ELA models clearly show that the lowering of ELAs in the southern Himalayas is largely due to a decrease in summer temperatures, and that an increase in monsoonal precipitation accounts for less than 30% of the total ELA changes. The decrease in summer temperatures is a dynamic response to the changes in solar insolation, resulting in both a decrease in incoming shortwave radiation at the surface due to an increase in cloudiness and an increase in evaporative cooling. In the western and northern zones of Central Asia, both ELA models show a rise in ELAs in response to a general increase in summer temperatures. This increase in temperatures in the more northern regions is a direct radiative response to the increase in summer solar insolation.

Introduction and motivation

In modern climate dynamics a central concept is that climate variability tends to be expressed in spatial patterns on a regional scale. Well-known examples of this are the El Nino-Southern Oscillation (e.g., Trenberth, 1997), the Pacific Decadal Oscillation (e.g., Mantua et al., 1997), and the Arctic Oscillation (e.g., Wallace and Gutzler, 1981). In past climates too, there are strong indications that climate changes occur in patterns, and no reason to suspect that they do not. Proper characterization and interpretation of past climate variability therefore requires a dense network of paleoclimate proxy records.

Glaciers are a particularly attractive paleoclimate proxy record for two reasons. First, geomorphic evidence of glacier advances is widespread across much of the Northern Hemisphere land masses. Second, glaciers are excellent recorders of properties of the atmosphere, retreating and advancing directly in response to changes in accumulation and ablation. Reconstructions of past glacier variability are some of the most useful records of paleoclimate. In fact, in many parts of the world, the glacier history is the primary descriptor of the climate history beyond the instrumental record, particularly where glacier deposits are widespread and confidently dated. This is true, for example, in the Pacific coast of the United States, South America, New Zealand, the European Alps, and Asia (e.g., Porter, 1977; Porter and Orombelli, 1985; Gillespie and Molnar, 1995; Lowell et al., 1995; Kaufman et al., 2004). Therefore, reconciling the glacier histories with the climatic variations that caused them is essential.

The glacier history of Central Asia provides a promising opportunity to distinguish between global and regional climate change. Until the early 1990's it was generally assumed that alpine glacier advances in Central Asia were synchronous with those of high-latitude ice sheets (e.g., Anderson and Prell, 1993; Emeis et al., 1995; Kuhle, 1998). As more extensive and reliable numerical dates have become available, it has become evident that alpine advances were not only asynchronous with glacier advances in other regions of the world, but also displayed regional variability within Asia itself (e.g., Gillespie and Molnar, 1995; Schafer et al., 2002; Finkel et al., 2003; Wei et al., 2006; Owen et al., 2008). The observed spatial patterns of glacier variability in Central Asia prompt three questions:

- Can we understand the relative importance of accumulation and ablation in controlling the mass balance of glaciers over large regions?
- Are the reconstructed spatial patterns of glacier response consistent with regional changes in climate?
- Do the reconstructed spatial patterns in glacier advances actually reflect patterns in climate change, or do they result from regional differences in the sensitivity of glacier mass balance to what might be relatively uniform changes in climate variables?

This paper focuses on reconciling the Holocene glacier record with climate. This is accomplished by analyzing a suite of general circulation models (GCMs) and quantifying glacier mass balance using two different mass-balance models. The first mass-balance

* Corresponding author.
E-mail address: summer_rupper@byu.edu (S. Rupper).

0033-5894/$ – see front matter © 2009 University of Washington. Published by Elsevier Inc. All rights reserved.
doi:10.1016/j.yqres.2009.03.007

model assumes ablation is proportional to temperature. The second is a surface energy- and mass-balance (SEMB) model that allows a test of glacier sensitivity to all climate changes seen in the GCMs.

Background

Central Asian glaciers

In order to simplify discussions of this geographically expansive region, we define "Central Asia" here as the region including the Himalayas, Tibetan Plateau, Mongolian Altai, Tien Shan, Pamir, Karakoram, and all regions contained within these mountainous boundaries (Fig. 1). Glaciers are found across Central Asia in a diverse range of climates, ranging from the intense monsoon of the southern Himalaya, to the extreme dryness of the eastern flank of the Karakorum and the extreme seasonal cycle (40°C) of the Mongolian Altai. It might be expected that these diverse climate regimes are likely to respond differently to uniform changes in climate forcing (e.g., summertime solar insolation). Since glaciers respond to the changes in climate, it is not surprising to find a diverse glacier history in these regions as well.

Glacier histories are often characterized in terms of equilibrium-line altitudes (ELAs). The ELA is the altitude on a glacier at which annual accumulation equals annual ablation. In general, a glacier advances if the ELA lowers and retreats if it rises. Changes in the ELA are considered one of the most useful glaciological measures for reconstructing climate changes (e.g., Porter, 1975; Paterson, 1999; Benn et al., 2005; Owen and Benn, 2005). The ELA can be compared directly from one region to the next. ELAs are also a more direct measure of climate than other glacier properties such as length, which depends on ice dynamics, bed geometry, and a myriad of other variables (Paterson, 1999). Changes in the ELA of any single glacier provide a history of the local climate. If those ELA variations are correlated across extensive glaciated regions, they can be interpreted as the history of the regional climate.

Some uncertainty obviously attends the ELA reconstructions (e.g., Owen and Benn, 2005). This uncertainty, and its impact on interpretation, will be addressed in more detail in the "Summary and discussion" section of this paper. We emphasize that for the purpose of this paper, it is not crucial for the changes in the ELA to be reconstructed precisely: we are primarily interested in relating the broader patterns of glacier response to the climate. This broader pattern is clear across Asia and the changes in an individual glacier's ELA are therefore less important.

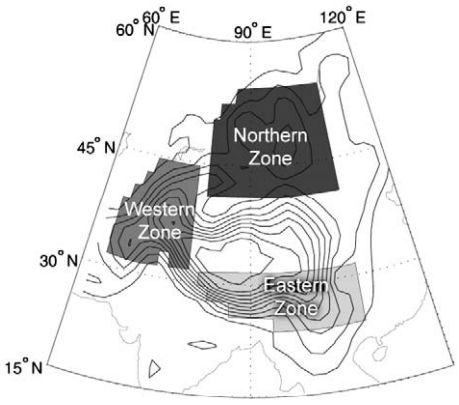

Figure 1. Central Asian zones: Shaded areas of gray represent the general outline of the eastern, western, and northern zones, as defined by the glacier history. These are the regions over which statistics are calculated (Table 1). Contours show the 500-m NCEP-NCAR reanalysis elevation increments; the zero contour is not shown. Coast lines are in gray. (Figure from Rupper and Roe, 2008.)

On the basis of the general pattern of ELA changes in Central Asia, we propose three general regions that capture the spatial and temporal variability of Pleistocene glaciers in Central Asia (Fig. 1) (Gillespie and Molnar, 1995; Gillespie et al., 2003; Owen et al., 2008). These three zones have distinct glacier histories, which are summarized briefly below.

The western zone extends from the Kyrgyz Tien Shan south to the Karakoram and east to central Tibet. In this region the largest advances occurred before the LGM (global last glacial maximum) (30–70 ka) with little evidence for large advances during the LGM itself for much of the region (~15–25 ka) (e.g., Phillips et al., 2000; Clark et al., 2001; Owen et al., 2002; Finkel et al., 2003; Koppes et al., in press; Barnard et al., 2004; Abramowski et al., 2006). In contrast, the glaciers in the northern zone (central Mongolia to the Tien Shan of Xinjiang, China) advanced during the LGM, synchronously with the high-latitude ice sheets, although there are published dates that push the western boundary of this zone west of the Mongol border (e.g., Shi, 2002; Gillespie et al., 2008). Although there is evidence for large pre-LGM and LGM advances in the southern Himalayas and Tibet (eastern zone), evidence for a large early Holocene (~9 ka) advance distinguishes it from the rest of Central Asia (e.g., Sharma and Owen, 1996; Richards et al., 2000; Schafer et al., 2002; Shi, 2002; Owen et al., 2003; Tschudi et al., 2003; Owen et al., 2005; Wei et al., 2006; Zhou et al., 2007). The pre-LGM glacier advance in the region is consistent with the strong sensitivity of these glaciers to local summertime temperatures and insolation swings, which were largest during the early part of the glacial cycle.

There are examples of smaller areas where the glacial history is different than the broader picture proposed above. For example, there is evidence of extensive glaciation in the Central Karakoram (part of the western zone) towards the end of the last glacial maximum (Seong et al., 2007). More generally, the ELA reconstructions available are still quite sparse and uncertainties in the exact timing of glacier advances are still quite large (e.g., Benn and Lehmkuhl, 2000; Owen et al., 2008). Therefore, the history of glaciations in these regions are not simple and smaller regions with homogeneous histories that differ from their neighbors cannot be ruled out (e.g., Seong et al., 2007; Owen et al., 2008). Nonetheless the sizes of the three regional zones are consistent with the spatial scale expected of major regional climate patterns, as found both for observations of the present climate and for models of past climate (discussed below and in Rupper and Roe, 2008). These zones are therefore a convenient framework for characterizing the glacier and climate histories.

We focus on explaining the relationship between Central Asian climate and early Holocene glacier history. We also place particular emphasis on understanding the advance of glaciers in the eastern zone. The early Holocene glacier history in the eastern zone is unusual as the glaciers advanced despite it being a time of a relative maximum in insolation during the Northern Hemisphere summer (e.g., Crowley and North, 1991).

Previous work

The climate of the mid-Holocene (6 ka) has been the focus of numerous modeling studies (e.g., Kutzbach and Gallimore, 1988; Dong et al., 1998; Hall and Valdes, 1997; Vettoretti et al., 1998; Joussaume et al., 1999; Braconnot et al., 2002; Bush, 2001, 2004). These studies consistently show that, in response to the changes in incoming solar insolation, the summer (JJA) temperatures in the interior of Central Asia (northern and western zones) increased by approximately 2 to 6°C compared to modern values (e.g., Joussaume et al., 1999). In climate model simulations, this increase in temperature enhances the land–sea temperature contrast, thereby intensifying the Indian summer monsoon. The models predict large increases in precipitation over India and the southern Himalaya (the eastern zone) in response to this increased intensity of the monsoon (Joussaume et al., 1999).

Table 1
Values are the mean change in summertime (Jun, Jul, Aug) temperature (ΔT_a), annual precipitation (ΔP), equilibrium-line altitude (ΔELA), and percent contribution of the change in ELA due to ΔT_a only to the total ΔELA (ΔELA:ΔT_a).

	Units	Eastern zone	Western zone	Northern zone
ΔT_a	°C	−1 (−0.5 to −2)	2 (2 to 4)	3 (2 to 6)
ΔP	mm yr^{-1}	500 (300 to 750)	−50 (−200 to 200)	90 (0 to 150)
ΔELA	m	−300 (−100 to −400)	400 (200 to 500)	450 (200 to 500)
ΔELA: ΔT_a	%	75 (70–85)	98 (90 to 100)	98 (95 to 100)

Values are the changes averaged over the individual zones (Fig. 1) in the ECHAM3 GCM simulation. Values in parentheses are the range in mean values for all GCM simulations.

Several studies have compared these climate changes to the available paleoclimate proxy data and noted the early Holocene glacier advance in the southern Himalaya (e.g., Kutzbach and Gallimore, 1988; Bush, 2002). Several papers focus specifically on explaining the Himalayan glacier advance (e.g., Benn and Owen, 1996; Finkel et al., 2003; Owen et al., 2003). All of these studies conclude that the advance of the glaciers in the southern Himalaya was a result of the increase in monsoonal precipitation during the Holocene.

However, glaciers respond to both annual precipitation and summer (melt-season) temperatures. Therefore the actual response of a glacier will depend on the changes in both of those variables as well as on the sensitivity of the glacier to each variable. For example, Kayastha et al. (1999) clearly show that glacier AX010 in the Nepalese Himalaya is sensitive to both temperature and precipitation. Yang et al. (2008) reconstruct glacier fluctuations in the southern Himalaya and southern Tibetan Plateau during the last two millennia. They conclude that temperature changes on centennial timescales controlled glacier fluctuations in the southern Himalayas and southern Tibetan Plateau. Given these examples from modern and past climates, both the increase in monsoonal precipitation and the increase in summer insolation must be accounted for in understanding the glacial history of the region.

We test the sensitivity of Central Asian glaciers to changes in both precipitation and insolation using a suite of general circulation model (GCM) simulations and two mass-balance models. The GCM simulations for 6 ka and the present day (discussed below) are used to describe the simulated changes in mid-Holocene temperatures and precipitation in the three zones. The climate model output is then used as input in the two mass-balance models. The first mass-balance model utilizes the traditional approach to estimating mass balance by assuming ablation is proportional to temperature. The second mass-balance model is a self-consistent surface energy-balance model (Rupper and Roe, 2008).

Holocene climate

The GCM data used in this study were acquired from the Paleoclimate Model Intercomparison Project (PMIP), which has archived output from multiple atmospheric GCM integrations with the appropriate conditions for several time periods, including the present day and 6 ka (Bonfils et al., 1998). The simulations for 6 ka are atmospheric GCMs forced by fixed sea surface temperatures. The temporal resolution of all GCMs is monthly; the spatial resolution is different for each model (typically model grids are between 2.5° and 5°). Although their spatial scales are coarse, the resolution of the models is adequate to compare climate and glacier sensitivities for the three generalized Central Asian regions of interest.

We analyze PMIP model output at 6 ka, which is somewhat offset from the timing of the largest Holocene glacier advances (~9 ka). The choice is made primarily because of the larger number model integrations that were made at 6 ka. No single model integration can be regarded as an accurate simulation of a past climate, and where agreement is found among different models it provides confidence in the robustness of the simulations. A small number of simulations were available at 9 ka, and in analyzing those we found no significant qualitative differences from the results presented here (in "Summary and discussion" section). Central Asia is far removed from the residual ice masses at 9 ka, and responds primarily to the local radiative balances. The suite of GCM output available at 6 ka provides a test of the sensitivity of Central Asian climate and glaciers to changes in incoming solar insolation. Moreover, dating uncertainties for the maximum Holocene glacier advances can be quite variable and large from one region to the next (e.g., Owen et al., 2008). Thus there is no single correct choice of optimum boundary conditions to choose for GCM simulations.

In our analysis of the climate models, we focus on precipitation and temperature because of the important link between these two variables and glacier mass balance. In presenting results, we give a table showing the spread in the climates simulated by the different models. For the most part there is a high degree of agreement between models in the simulated changes. In showing maps of the simulated changes, we focus therefore on one GCM, ECHAM3. Importantly, the consistency between model simulations suggests robustness of the climate response to changes in insolation forcing.

Summertime (JJA) temperatures increase by 2 to 6°C as compared to the modern values in the northern and western zones (Table 1, Fig. 2). This is a direct result of the increase in summer insolation in these regions, and is consistent with the continentality of these areas. In contrast to this, the temperature in the eastern zone actually decreased by 0.5 to 2°C despite the increase in summertime insolation. As we will show in the "ELA calculations" section, this decrease in temperatures is important for explaining the glacier response in the southern Himalaya. The reasons for this response are examined closely in the "Explaining the temperature changes" section.

The changes in precipitation in response to the increase in incoming solar insolation are also different in the three regions (Fig. 3). In the northern zone the change in precipitation at 6 ka as compared to present day was negligible to slightly positive (0 to 150 mm yr^{-1}) (Table 1). The tendency of the models towards a slight

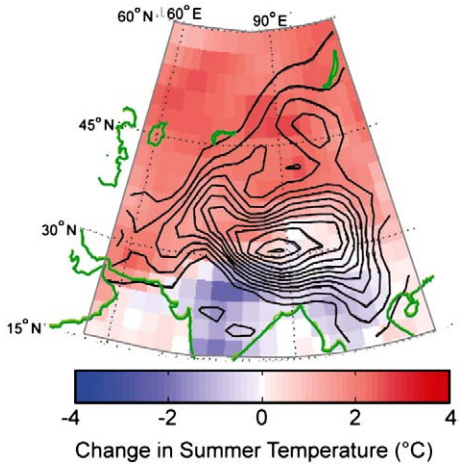

Figure 2. Change in summertime (Jun, Jul, Aug) air temperature (°C) for 6 ka compared to present day. Contours show the 500-m NCEP-NCAR reanalysis elevation increments; the zero contour is not shown. Coast lines are in green. Elevation and contour intervals are the same for all subsequent figures.

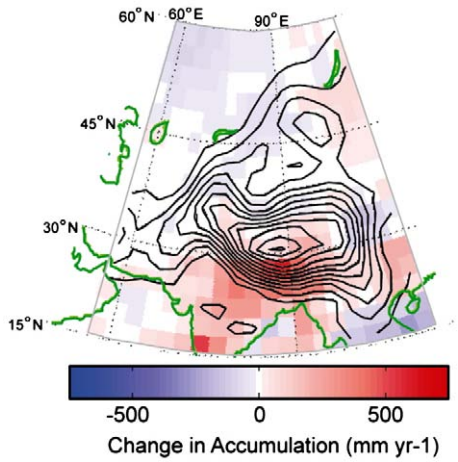

Figure 3. As in Figure 2, but for a change in annual accumulation (mm yr^{-1}).

increase in precipitation may be due to the increase in temperature: for constant relative humidity, moisture content increases with temperature, as given by the Clausius–Clapeyron relation, though GCMs typically show precipitation increases with temperature, but at a rate somewhat less than the relation would imply (e.g., Wallace and Hobbs, 2005; Allen and Ingram, 2002). In the western zone, the changes in precipitation are also small in comparison to the monsoon regions, but quite variable; even the sign of the changes is not consistent between models (−200 to 200 mm yr^{-1}) (Table 1). We have not diagnosed the reasons for this variability in detail, though it is perhaps due to model differences in the response of springtime precipitation associated with storms originating in the Mediterranean (e.g., Hoskins and Hodges, 2002). However, we will show below that the glaciers are not sensitive to these changes in precipitation. Therefore, this inter-model variability does not change our main conclusions. Compared to the small changes in precipitation in the northern and western zones, changes in precipitation in the eastern zone are substantial, ranging between 300 to 750 mm yr^{-1}, increasing in all models. These results agree with other studies which also show an increase in precipitation at 6 ka as a result of an increase in monsoon intensity and/or duration (e.g., Joussaume et al., 1999).

There are two important results from the analysis of precipitation and temperature changes in Central Asia. First, with the exception of precipitation changes in the western zone, all the GCMs show broadly similar results for precipitation and temperature changes. This reinforces confidence that the GCM simulated climate changes are a robust response of the climate to the changes in insolation forcing. Second, the GCMs show spatial variability in the temperature and precipitation changes across Central Asia in response to a relatively uniform increase in incoming solar insolation. This suggests that even a uniform change in forcing, such as increasing greenhouse gases, should result in spatial patterns in climate response. Because glaciers respond to changes in temperature and precipitation, this spatial variability in temperature and precipitation changes should result in corresponding patterns of glacier variability across Central Asia. The next section focuses on whether the patterns in climate are sufficient to explain the geologic data.

ELA calculations

To understand the impact of the modeled climate changes on glacier mass balance, the GCM output is converted into ELA changes, using two different methods. The first, discussed below, is an ELA perturbation model following Ambach and Kuhn (1985), modified to use the positive degree-day (PDD) model for ablation, following Braithwaite (1995). The second model is a surface energy-balance model (Rupper and Roe, 2008), which is discussed briefly in the following subsection on "modeled ELA changes: PDD approach." Both models solve for the change in ELA for a given change in climate.

PDDs are the sum of daily mean air temperatures (T_a) that are above zero.

$$\mathrm{PDD} = \sum H(T_a), \tag{1}$$

where H is equal to 0 for $T_a \leq 0$ and is equal to T_a for $T_a > 0$; the sum is taken over the calendar year. Thus PDD has units of °C days. We determine PDDs using the monthly mean GCM output by calculating the daily mean air temperature (T_a) as

$$T_a = \overline{T}(z) + T_{amp}\cos\left(2\pi\frac{t}{365}\right). \tag{2}$$

$\overline{T}$ is the mean annual air temperature, t is the day of the year, and T_{amp} is the amplitude in the seasonal cycle in air temperature determined using the monthly GCM output. Total ablation is then equal to PDD times a melt factor. The results presented below are for a melt factor equal to 10 mm $°C^{-1}$ day^{-1}, the midpoint of the modeled and empirically-derived range in melt factors from Rupper and Roe (in press) and measured values (Kayastha et al., 1999, Zhang et al., 2006). Although the magnitude of the modeled ELA changes is affected by the choice of melt factor, the basic pattern of the ELA response does not change.

In Eq. (3), accumulation (A_c) equals ablation (A_b) at the ELA. For a change in A_c or A_b a first-order Taylor Series expansion in the vertical direction can be used to calculate the change in the ELA that would result from a change in accumulation or temperature.

$$\Delta A_c = \Delta A_b + \frac{\partial A_b}{\partial z}\Delta z \tag{3}$$

where Δ refers to the change from a reference climate.

The input variables on the right-hand side of Eq. (3) are the change in ablation and the gradient in ablation. The vertical gradient in ablation is calculated by: (a) varying $\overline{T}$ about the climatological temperature lapse rate, (b) calculating the change in ablation at the different elevations along the lapse rate (using Eqs. (1) and (2)), and (c) dividing by the change in elevation. The climatological lapse rate is calculated using NCEP-NCAR reanalysis annual average air temperatures at 750 and 500 hPa (Kalnay et al., 1996). The lapse rates are then interpolated to the same grid as the GCMs.

Strictly, the left-hand side of Eq. (3) (ΔA_c) should include both the gradient in accumulation about the ELA and the change in accumulation (e.g., Ambach and Kuhn, 1985). However, the gradient in accumulation can be neglected for typical ELA changes, so is not included in the ELA calculations. Therefore, ΔA_c is simply the change in accumulation.

ELA changes are calculated for the given changes in climate across the entire model domain. We are therefore effectively asking "if there were a glacier at this grid point, what would its change in ELA be?" Given this approach to estimating ELA changes, and the coarse resolution of the GCM grid (typically between 2.5° to 5°), two issues arise. First, the smoothed topography makes it difficult to differentiate between precipitation and snow. We assume that precipitation would all be snow, thus A_c equals total annual precipitation. This errs on the side of maximizing sensitivity to model accumulation, but alternative assumptions would not change our basic results. Second, Anders et al. (2006) show that precipitation in the Himalayas varies significantly on scales much smaller than the GCM grid resolution. These GCMs therefore do not capture patterns of orographic precipitation adequately.

We test the sensitivity of our results to the grid scale by calculating the ELA using model output and data at different resolutions. In particular, we use the algorithm (modified to use the PDD approach to

estimate ablation) discussed in the subsection "Modeled ELA changes: Energy-balance approach" to seek the position of the ELA using temperature and precipitation from the present-day GCM simulations. We do the same using the higher resolution precipitation and temperature data from Legates and Willmott (1990a, 1990b). While the 0.5°-grid resolution is still too coarse to capture orographic precipitation, it does provide a means to test the sensitivity of the results to changes in spatial resolution. The basic pattern in ELAs is similar regardless of resolution. The effect of smaller-scale patterns of orographic precipitation is addressed in Huybers and Roe (2008).

Modeled ELA changes: PDD approach

The pattern of ELA changes calculated from Eq. (3) is similar for all GCMs. In Table 1, we summarize the results for all models; in the figures discussed below, we show results only for one GCM, the ECHAM3.

The simulated changes in precipitation and temperature at 6 ka as compared to the present day produces a pattern in ELA changes across Central Asia (Fig. 4). In the eastern zone, the change in climate results in a lowering of ELAs by approximately 300 m and a lifting elsewhere by 200 to 500 m. If only precipitation changes are included (i.e., temperatures are held fixed), ELAs in the east are lowered by only 75 m (Figs. 4a, b). Thus changes in precipitation account for less than 30% of the total modeled change in ELAs in the eastern zone. In the northern and western zones, changes in precipitation account for even less (at most 5%) of the total change in ELAs. Thus, for the range of changes in temperature and precipitation predicted by the GCMs, ELAs in all regions are most sensitive to changes in temperature; and except in the eastern zone, precipitation changes are nearly negligible. In all zones, the largest uncertainty in the calculated ELA changes is the ablation term (i.e., the value chosen for the melt factor). However, for the full range of melt factors the dominance of the temperature pattern still applies.

The calculated ELA changes predict that glaciers would have been bigger during the Holocene compared to the present day in the eastern zone, while glaciers in the north and west were smaller. This is consistent with the paleoclimate record, in which geologic evidence shows a significant advance in the eastern zone during the Holocene and glaciers equal to or smaller than modern glaciers in the north and west (e.g., Sharma and Owen, 1996; Richards et al., 2000; Schafer et al., 2002; Shi, 2002; Owen et al., 2003; Tschudi et al., 2003; Owen et al., 2005; Wei et al., 2006; Zhou et al., 2007).

Modeled ELA changes: Energy-balance approach

The simple PDD method assumes that ablation is directly related to temperature. Physically, of course, it is the net heat input that is actually responsible for the melting or sublimation of snow and ice. A surface energy-balance model is needed to calculate the heat available for ablation. Such models are self-consistent representations of all the surface heat fluxes, and have often been used to study the energy balance at particular glaciers (e.g., Kayastha, 1999; Molg and Hardy, 2004). For the application to regional-scale climate patterns, we use the surface energy- and mass-balance model (SEMB model) presented in Rupper and Roe (2008). Applying the model to this study serves two purposes. First, it provides a check on the answers derived from the PDD method. Second, the analysis of the surface energy fluxes

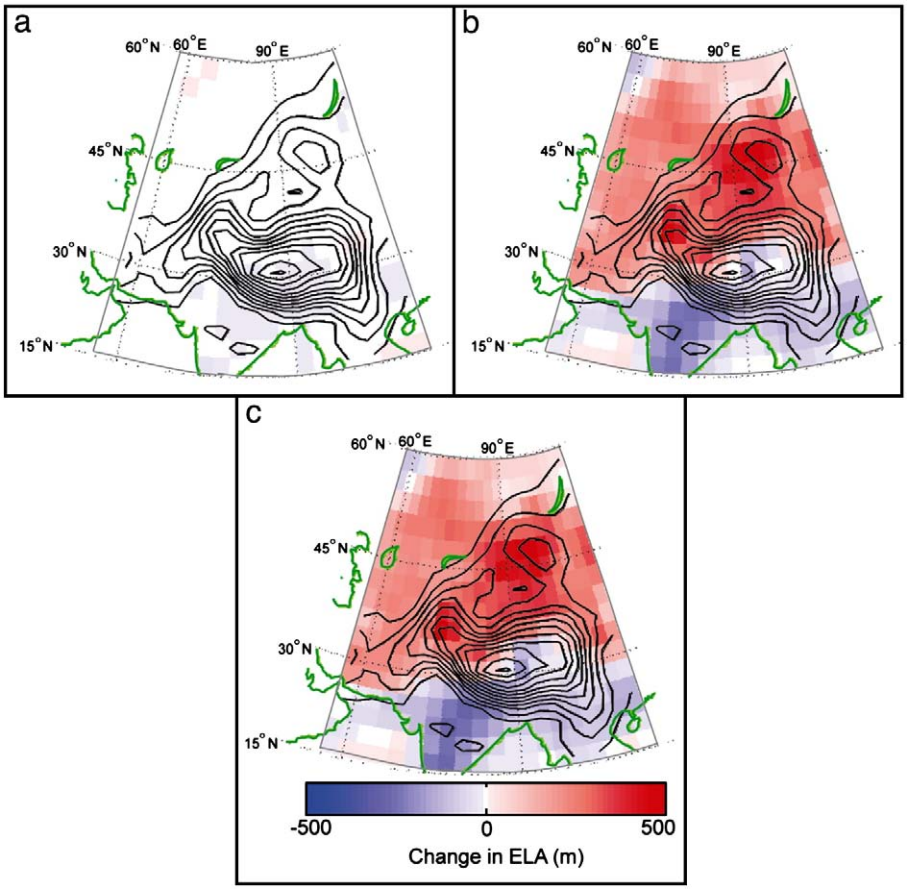

Figure 4. Change in equilibrium-line altitude (m) at 6 ka as compared to the present day calculated using the PDD approach. ELA changes are for a: (a) change in accumulation only, (b) change in ablation only, and (c) change in both temperature and accumulation. These figures illustrate the result that the ELAs in Central Asia are most sensitive to changes in temperature.

leads to important new insights that help explain the cooling of temperatures in the eastern zone.

A complete description of the SEMB model is given in Rupper and Roe (2008). Briefly, for a specified climate forcing at a given grid point, the SEMB model seeks the altitude at which a glacier surface would be in both mass and energy balance over the annual cycle. By definition, this is the ELA. The inputs from the climate model are the annual cycles in downwelling shortwave radiation, air temperature (at the climate model surface), wind, atmospheric pressure, and relative humidity. The SEMB model parameterizes the surface albedo and the downwelling longwave radiation. Sensible and latent heat fluxes are calculated in terms of the specific humidity, wind speed, assumed roughness lengths, and temperature difference between the surface and the overlying air.

The energy-balance algorithm seeks a surface temperature for a given air temperature that balances the absorbed shortwave radiation at the surface. When the surface temperature is less than zero, sublimation occurs. When the surface temperature is greater than or equal to zero, the surface temperature is reset to zero and the energy balance recalculated. The excess energy is then used to calculate the total melt. In this way the total ablation is calculated for a given mean annual air temperature. In the mass-balance algorithm, the model seeks the elevation at which the mean annual air temperature results in a total annual ablation (calculated using the energy-balance method above) that exactly equals the total annual accumulation.

The SEMB model involves some significant simplifying assumptions, but it does capture the behavior of how the different surface energy fluxes adjust to balance the radiative forcing. Rupper and Roe (2008) show that the framework is suitable for characterizing the dependence of the ELA on regional climate patterns and can, for example, identify regions where sublimation or melt dominate the mass balance at the ELA. Such results give insight into which atmospheric variables the ELA is most sensitive to.

We use monthly time steps over the annual cycle, which are sufficient to represent the typical magnitude of the observed energy fluxes at glacier surfaces, and their seasonal cycles (Rupper and Roe, 2008). We use the output from the climate models at the present day and 6 ka to calculate the change in ELA predicted by the model, and to analyze the reasons for the predicted change.

We present the results from the ECHAM3 model for comparison to the PDD results presented above. As with the PDD approach, the change in climate at 6 ka as compared to the present day produces a pattern in ELA changes across Central Asia (Fig. 5a). The overall pattern in ELA changes using the surface energy-balance approach is generally very similar to that of the PDD approach. Where the two methods disagree is in regions where the ablation is dominated by the sublimation term. This includes small portions of the northern and western zones. ELA changes calculated using the SEMB model are much larger in these regions than elsewhere in Central Asia. When sublimation dominates the mass balance, large changes in surface temperature are necessary for sublimation alone to bring the system back into mass balance, which results in large changes in ELAs. Therefore sublimation regions are very sensitive to even small changes in precipitation. ELAs in regions dominated by sublimation, calculated using the PDD approach, should be interpreted with caution (see Rupper and Roe, 2008, for a detailed discussion of the reasons for melt versus sublimation).

To facilitate further comparison of the surface energy-balance model results to the PDD method, the ELA changes averaged over each of the three zones are presented. In the eastern zone, the change in climate results in a lowering of ELAs by approximately 350 m. Elsewhere in Central Asia (excluding sublimation regions), ELAs increase by approximately 450 m. The relative importance of ablation versus accumulation in determining the ELA changes can be analyzed by computing the changes in ELAs while neglecting the change in precipitation (Fig. 5b). That is, ELA changes are calculated for a change

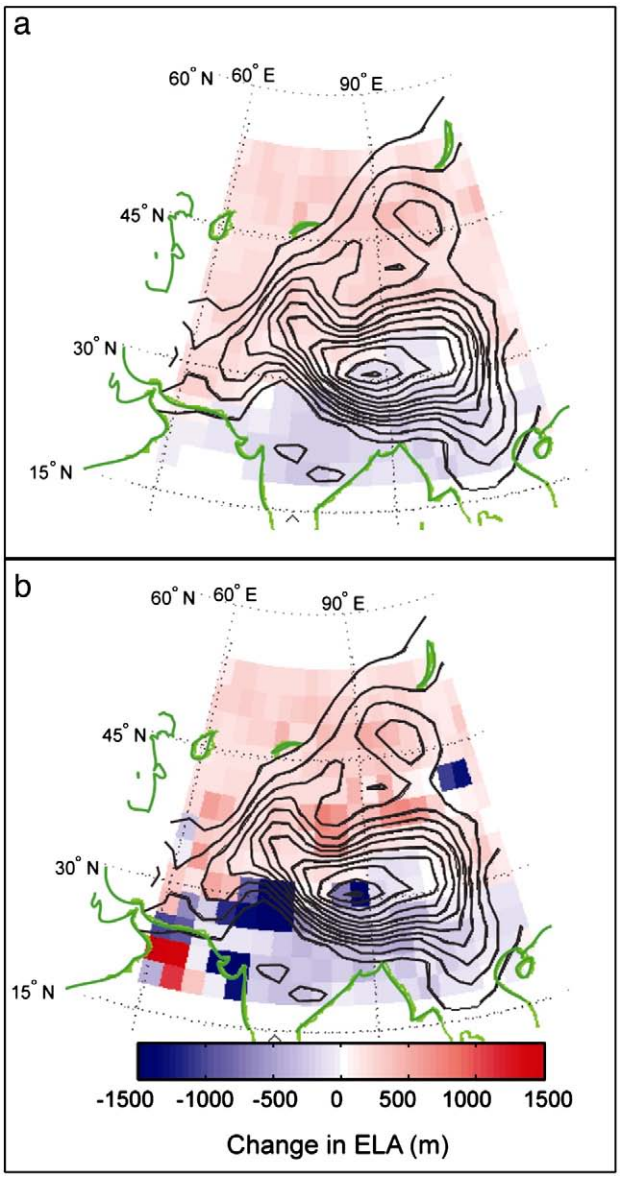

Figure 5. Change in ELA (m) at 6 ka minus the present day, calculated using the surface energy- and mass-balance model after Rupper and Roe (2008). Panel (a) is the change in ELA for a change in ablation only. Panel (b) is the change in ELA for the simulated changes in both accumulation and ablation. (Note scale is different than in Fig. 4.)

in ablation only. In this case, the ELAs in the east lower by approximately 250 m, more than 70% of the total ELA change. Thus changes in precipitation account for less than 30% of the total change in the ELA (similar to the results reported for the PDD approach). Outside of the eastern zone and excluding the sublimation-dominated regions, changes in precipitation account for at most 5% of the total change in the ELA (again comparable to the results using the PDD method). In contrast to these melt-dominated regions, sublimation-dominated regions are very sensitive to changes in precipitation with precipitation changes accounting for 50% to 80% of the total ELA change.

The results suggest that where melting dominates, the PDD approach adequately captures the physics included in the full energy-balance model. Where sublimation dominates, however, the PDD approach greatly underestimates the sensitivity of the ELA to small changes in precipitation. These results indicate that for the typical changes in atmospheric variables predicted by the GCM's, glaciers in the melt-dominated regions are most sensitive to those changes that conspire to change temperature. Therefore the surface

energy-balance model confirms the result that the pattern in ELA changes across Central Asia (for the 6 ka minus the present-day results) is primarily a result of the pattern in temperature changes, with the exception of the sublimation-dominated regions.

Explaining the temperature changes

Holocene climate reconstructions from paleoclimate proxy records (mainly sediment cores and speleothems) show multiple episodes of cooler temperatures during the early to mid-Holocene (e.g., Wang et al., 2005; Wang and Zhu, 2005; Rashid et al., 2007; Xiang et al., 2007). The GCM simulations used in this study cannot capture such millennial-scale variability; therefore, the timing of short-term cooling events cannot be compared directly to the model results. However, in a general way, these reconstructions do support the model results — that temperatures decreased during the early (9 ka simulation) to mid-Holocene (6 ka simulations) in and around the eastern zone despite an increase in incoming solar insolation at the top of the atmosphere.

To our knowledge, the mechanisms giving rise to the decrease in temperature in the eastern zone has not previously been addressed in the context of the paleoclimate reconstruction. Since this decrease plays an important role in the modeled ELA changes, it is important to understand the physical causes. Insight into these temperature changes is gained through a discussion of modern variability in monsoonal temperatures and precipitation, and analysis of the radiation balance in the GCM integrations.

Both the seasonal cycle and the interannual variability of the modern Indian monsoon suggest a reason for the model results of lower temperatures over the eastern zones at 6 ka. When the monsoon rains begin every year, temperatures lower over India, and years with a strong monsoon are also years with greater than average cloudiness and below-average surface air temperature (e.g., Ramanathan, 1987; Collins et al., 1996; Wilcox and Ramanathan, 2001). The climate model output at 6 ka suggests that an analogous situation occurred during the mid-Holocene. All models predict increased cloudiness (as well as albedo) along with the decreased temperatures at 6 ka relative to the present day (Fig. 6a).

The connection between the changes in radiation and the temperature response at the surface can be seen by analyzing the terms in the surface energy balance. As the results are again broadly similar for all GCM's, the results for one model, ECHAM3, are presented here. Figure 6b shows the difference between 6 ka and present-day shortwave radiation at the surface along with the change in cloud fraction (Fig. 6a); the patterns in shortwave radiation and cloud fraction are very similar. Figures 7a–c present the changes in surface longwave radiation and surface sensible and latent heat fluxes. Together these figures show that in the central and western portion of the Himalaya there is a decrease in both shortwave radiation (-40 W m^{-2}) and latent heat (-45 W m^{-2}). Therefore, both an increase in cloud fraction and an increase in evaporation contribute to the surface cooling. In the far eastern portion of the Himalaya there is no significant change in the latent heat, only in the shortwave radiation. Thus, the cooling in the far eastern Himalaya can be attributed to the decrease in shortwave radiation (-50 W m^{-2}) due to the increased albedo (increased cloud fraction) compared to the present day. Therefore, the surface cooling across the eastern zone is due in part to an increase in evaporation as well as an increase in cloudiness. Finally, in the northern and western zones, the increase in summer temperatures is a direct result of the increased shortwave radiation reaching the surface due to orbital changes (30 W m^{-2} summertime average).

In summary, these results suggest that the advance of glaciers in the southern Himalaya is a result of a combination of factors. Enhanced monsoon intensity and/or duration led to an increase in precipitation as well as a decrease in temperature via increased cloud fraction (decreased shortwave radiation) and evaporation. Thus, glaciers in the eastern region are influenced by changes in the monsoons and the associated changes in both temperature and precipitation. These results contradict previous work suggesting that early to mid-Holocene glacier advances in the southern Himalaya were due to increased precipitation only. The lack of glacier advance in the northern and western zones is due to the large increase in average summer temperatures, a direct result of the increase in incoming summer insolation, consistent with other results showing a strong sensitivity of continental climates to changes in radiation (e.g., Felzer et al., 1995).

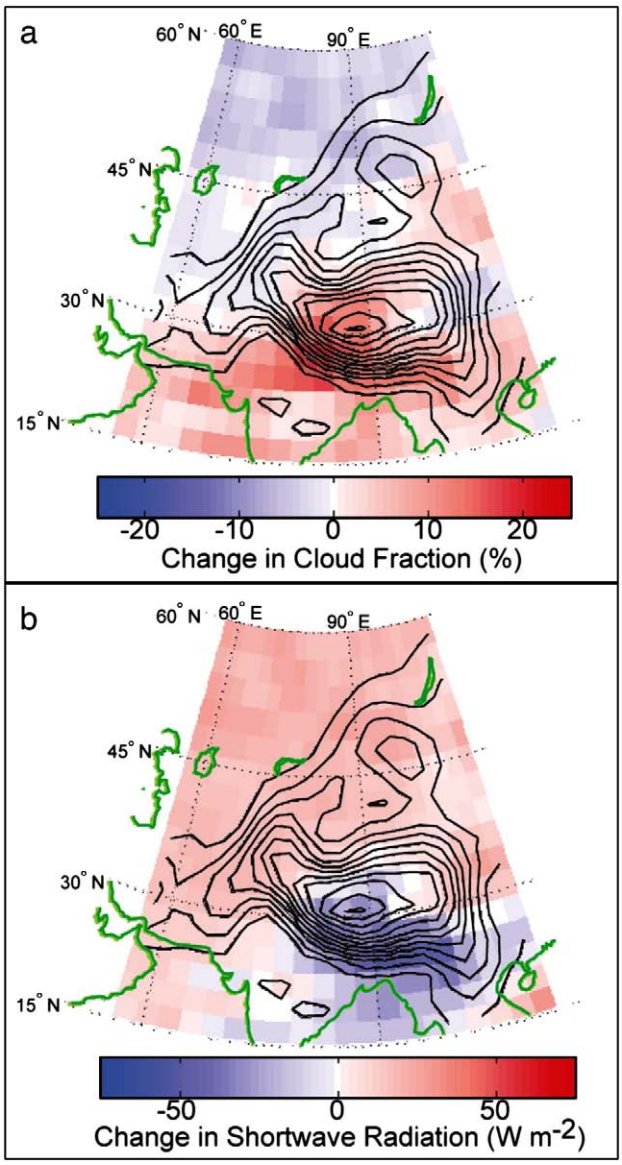

Figure 6. Change in (a) cloud fraction (%) and (b) shortwave radiation (W m^{-2}) at the surface for 6 ka as compared to the present day.

Summary and discussion

Central Asian glacier history provides a unique opportunity to reconcile regional-scale glacier changes with the climate mechanisms driving them. In particular, the advance of glaciers in the southern Himalaya in the early Holocene (9 ka) is in contrast to the smaller alpine glaciers in the western and northern regions of Central Asia (e.g., Gillespie and Molnar, 1995; Gillespie et al., 2003, 2008; Koppes et al., 2008).

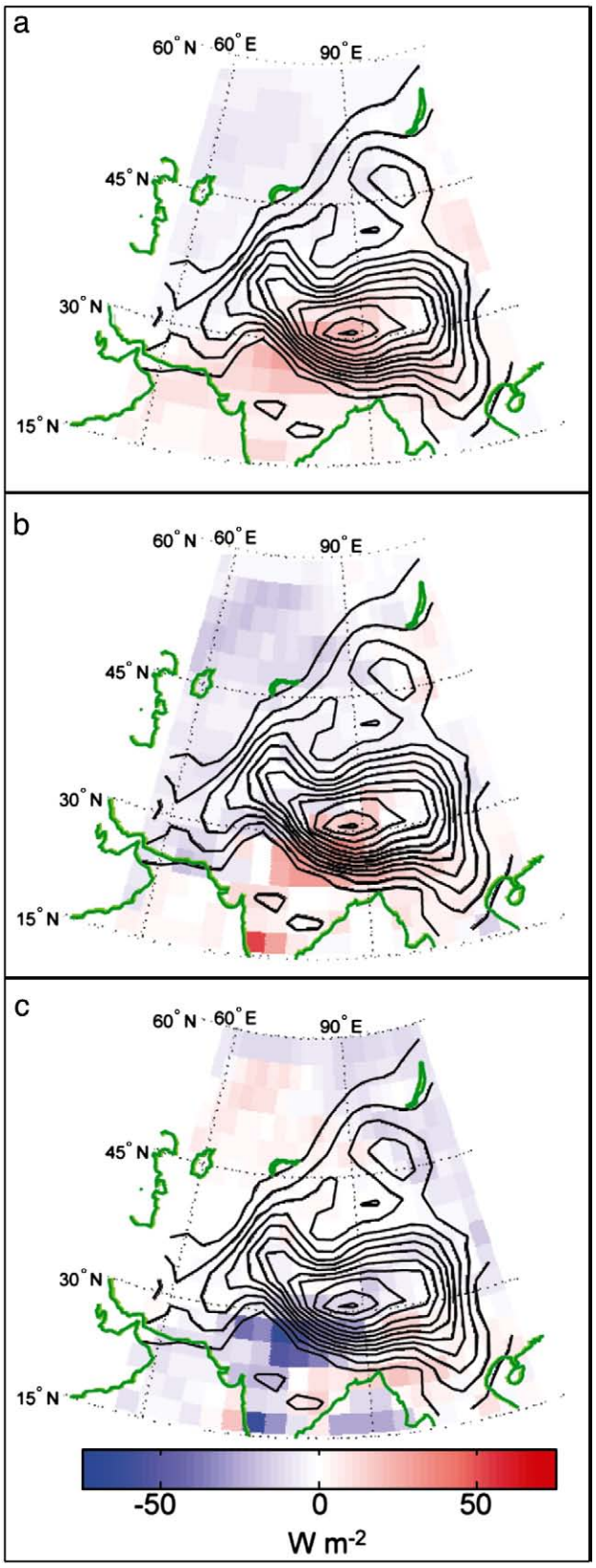

Figure 7. Change in surface (a) longwave radiation, (b) sensible heat flux, and (c) latent heat flux (all in W m^{-2}) for 6 ka as compared to the present day.

Previous studies attribute this southern Himalayan Holocene glacier advance to an increase in monsoonal precipitation (e.g., Benn and Owen, 1998; Bush, 2002; Finkel et al., 2003). Although a substantial increase in precipitation is evident during the early and mid-Holocene in GCM simulations (e.g., Joussaume et al., 1999), our results show that this is only a part of the story. We use two different mass-balance models to quantify the change in ELA for simulated changes in mid-Holocene climate. The first of these models uses a positive degree-day approach to estimate ablation (Braithwaite, 1995) and a modified version of the Ambach and Kuhn (1985) ELA perturbation method to calculate changes in ELA. As such, this model was used to assess the relative importance of temperature and precipitation on ELA changes in Central Asia. The second model is a self-consistent surface energy- and mass-balance model that incorporates changes in all relevant atmospheric variables (Rupper and Roe, 2008). Eighteen GCM simulations using boundary conditions appropriate for the present day and 6 ka were acquired from PMIP and used as input in the ELA models. While assumptions and simplifications in the model formulations must be made, due in large part to the coarse grid (2.5° to 5°) and temporal resolution (monthly) of the GCM output, these were found not to change the main conclusions significantly. The pattern in ELA changes using both models were consistent for those regions where melt dominates total ablation, suggesting the PDD approach is appropriate in melt regions.

Both ELA models clearly show that the lowering of ELAs in the southern Himalayas, a region dominated by melt, is largely due to a decrease in summer temperatures during the early Holocene, and that the increase in precipitation accounts for, at most, 30% of the total ELA changes. In the melt-dominated regions of the western and northern zones, both ELA models show a rise in ELAs in response to a general increase in temperatures. Importantly, these results suggest that there is regional variability in the climate's response to the increase in Northern Hemisphere summer insolation, and that the regional variability in glacier changes in Central Asia is largely explained by the resulting temperature pattern in the melt-dominated regions. Sublimation dominates the ablation in portions of the northern and western zones. In these sublimation-dominated regions, the mass and energy-balance model shows that ELAs are acutely sensitive to changes in precipitation. Thus, the sensitivity of the ELAs to changes in climate depends on the dominant ablation process.

Through a detailed evaluation of the energy balance at the surface, we were able to explain the pattern in temperature changes in Central Asia. The increase in summer temperatures in the more northern regions of Central Asia is a direct radiative response to the increase in solar insolation at 6 ka, and is consistent with other studies showing temperatures in continental interiors slaved to radiation changes (e.g., Felzer et al., 1995). The temperature decrease in the more southern regions, on the other hand, is a dynamic response to the increase in temperatures in the interior. In particular, the increase in land–sea temperature contrast intensifies the monsoonal circulation. This results in an increase in precipitation as well as a substantial increase in cloudiness over the southern region. The decrease in summer temperatures is the result of both a decrease in shortwave radiation due to the increase in cloudiness (and a resulting increase in albedo) and an increase in evaporative cooling.

The results presented in this study are for climate changes at 6 ka while the largest Holocene glacier advances occurred earlier in the Holocene, ~9 ka. It is important to discuss the validity of the results in light of this time discrepancy. The boundary conditions around 9 ka were similar to that for 6 ka but with small remnants of the ice sheets remaining at higher latitudes, and larger increases in Northern Hemisphere summer insolation. We compared our results to one GCM simulation under boundary conditions appropriate for 9 ka, the CCM0 AGCM. The patterns in climate and ELA changes for 9 ka were very similar to those for 6 ka, but with larger changes in both. The mechanisms giving rise to the climate and ELA changes are also the same for 9 ka and 6 ka. Therefore, it is reasonable to use the PMIP suite of GCM simulations for 6 ka to understand the early Holocene glacier advances.

The consistency between all GCMs reinforces confidence that the model results are a robust response of the climate to the changes in insolation forcing. In the case for Central Asia, spatial patterns in climate occur in response to a relatively uniform increase in solar insolation at the top of the atmosphere. The patterns in glacier advances across Central Asia are a result of the spatial variability in the climate response. This suggests that spatial patterns in climate and glaciers should be expected even in cases where there is a uniform change in forcing (e.g., increasing CO_2). In contrast to previous work, our results strongly suggest that the advance of glaciers in the southern Himalaya is a result of a combination of factors, not just increased precipitation. Finally we note that when climate modeling can be employed with sufficient confidence, and when high-quality and well-dated glacier records are available, the approach taken here can be applied to exploring the climatic causes of past glacier variations at other times and locations.

These glaciers and their history represent a case study of a more general issue in paleoclimate research. The results emphasize the critical importance of having a good physical model to test the sensitivity of a given climate proxy to climate change. Such models are essential to establish whether a proposed mechanism is, firstly, a unique explanation for a given record and secondly, of sufficient magnitude to impart the recorded signal.

Acknowledgments

We thank David Battisti, Michele Koppes, Chris Bretherton, and Eric Steig for many insightful discussions that led to the exposition of this paper. We also thank Tom Morris and Steve Nelson for valuable suggestions on earlier drafts of the manuscript, Boa Yang and Frank Lehmhukl for thoughtful and constructive reviews, and Lewis Owen the editor. GHR acknowledges support from NSF continental dynamics grant #0409884.

References

Abramowski, U., Bergau, A., Seebach, D., Zech, R., Glaser, B., Sosin, P., Kubik, P.W., Zech, W., 2006. Pleistocene glaciations of Central Asia: results from Be-10 surface exposure ages of erratic boulders from the Pamir (Tajikistan), and the Alay-Turkestan range (Kyrgyzstan). Quaternary Science Reviews 25 (9–10), 1080–1096.

Allen, M.R., Ingram, W.J., 2002. Constraints on future changes in climate and the hydrological cycle. Nature 419, 224–232.

Ambach, W., Kuhn, M., 1985. Accumulation gradients in Greenland and mass balance response to climatic changes. Z Gletscherkd Glazialgeol 21, 311–317.

Anders, A., Roe, G., Hallet, B., Montgomery, D., Finnegan, N., Putkonen, J., 2006. Spatial patterns of precipitation and topography in the Himalaya, In Willett, S.D., Hoovius, N., Brandon, M.T., and Fisher, D.M., eds., Tectonics, Climate and Landscape Evolution. GSA Special Paper 398, Chapter 3, pp. 39–53.

Anderson, D.M., Prell, W.L., 1993. A 300 kyr record of upwelling off Oman during the late Quaternary — evidence of the Asian southwest monsoon. Paleoceanography 8 (2), 193–208.

Benn, D.I., Owen, L.A., 1998. The role of the Indian summer monsoon and the mid-latitude westerlies in Himalayon glaciation: review and speculative discussion. Journal of the Geological Society 155, 353–363.

Benn, D.I, Lehmkuhl, F., 2000. Mass balance and equilibrium-line altitudes of glaciers in high-mountain environments. Quaternary International 65–6, 15–29.

Benn, D.I., Owen, L.A., Osmaston, H.A., Seltzer, G.O., Porter, S.C., Mark, B., 2005. Reconstruction of equilibarium-line altitudes for tropical and sub-tropical glaciers. Quaternary International 138, 8–21.

Barnard, P., Owen, L., Finkel, R., 2004. Style and timing of glacial and paraglacial sedimentation in a monsoon-influenced high Himalayan environment, the upper Bhagirathi valley, Gavhwal Himalaya. Sedimentary Geology 165, 199–221.

Bonfils, C.J., Lewden, D., Taylor, K.E., 1998. Documentation of the PMIP models. PMCI Report.

Braconnot, P., Loutre, M.F., Dong, B., Joussaume, S., Valdes, P., 2002. How the simulated change in monsoon at 6 ka BP is related to the simulation of the modern climate: results from the Paleoclimate Modeling Intercomparison Project. Climate Dynamics 19 (2), 107–121.

Braithwaite, R.J., 1995. Positive degree-day factors for ablation on the Greenland ice-sheet studied by energy-balance modeling. Journal of Glaciology 41 (137), 153–160.

Bush, A.B.G., 2001. Pacific sea surface temperature forcing dominates orbital forcing of the Early Holocene monsoon. Quaternary Research 55 (1), 25–32.

Bush, A.B.G., 2002. A comparison of simulated monsoon circulations and snow accumulation in Asia during the mid-Holocene and at the Last Glacial Maximum. Global and Planetary Change 32 (4), 331–347.

Bush, A.B.G., 2004. Modelling of late Quaternary climate over Asia: a synthesis. Boreas 33 (2), 155–163.

Collins, W.D., Valero, F.P.J., Flatau, P.J., Lubin, D., Grassl, H., Pilewskie, P., Spinhirne, J., 1996. The radiative effects of convection in the Tropical Pacific. Journal of Geophysical Research 101 (D10), 14999–15012.

Crowley, T.J., North, G.R., 1991. Abrupt climate change and extinction events in earth history. Science 240 (4855), 996–1002.

Dong, G.R., Wang, G.Y., Li, X.Z., Chen, H.Z., Jin, J., 1998. Palaeomonsoon vicissitudes in eastern desert region of China since last interglacial period. Science in China Series D-Earth Sciences 41 (2), 215–224.

Emeis, K.C., Anderson, D.M., Doose, H., Kroon, D., Schulzbull, D., 1995. Sea-surface temperatures and the history of monsoon upwelling in the northwest Arabian Sea during the last 500,000 years. Quaternary Research 43 (3), 355–361.

Felzer, B., Oglesby, R.H., Shao, H., Webb, T., Hyman, D.E., Prell, W.L., Kutzbach, J.E., 1995. A systematic study of GCM sensitivity to latitudinal changes in solar-radiation. Journal of Climate 8 (4), 877–887.

Finkel, R.C., Owen, L., Barnard, P., Caffee, M., 2003. Beryllium-10 dating of Mount Everest moraines indicates a strong monsoon influence and glacial synchroneity throughout the Himalaya. Geology 31 (6), 561–564.

Gillespie, A., Molnar, P., 1995. Asynchronous maximum advances of mountain and continental glaciers. Reviews of Geophysics 33 (3), 311–364.

Gillespie, A., Rupper, S., Roe, G., 2003. Climatic interpretation from mountain glaciations in Central Asia. Geological Society of America, Abstracts with Program 35 (6).

Gillespie, A.R., Burke, R.M., Komatsu, G., Amgalan Bayasgalan, A., 2008. Late Pleistocene glaciers in Darhad Basin, northern Mongolia. Quaternary Research 69 (2), 169–187.

Hall, N.M.J., Valdes, P.J., 1997. A GCM simulation of the climate 6000 years ago. Journal of Climate 10 (1), 3–17.

Hoskins, B.J., Hodges, K.I., 2002. New perspectives on the Northern Hemisphere winter storm tracks. Journal of the Atmospheric Sciences 59 (6), 1041–1061.

Huybers, K., Roe, G.H., 2009. Spatial patterns of glaciers in response to spatial patterns in regional climate. Journal of Climate 22 (17), 4606–4620.

Joussaume, S., Taylor, K.E., Braconnot, P., Mitchell, J.F.B., Kutzbach, J.E., Harrison, S.P., Prentice, I.C., Broccoli, A.J., Abe-Ouchi, A., Bartlein, P.J., Bonfils, C., Dong, B., Guiot, J., Herterich, K., Hewitt, C.D., Jolly, D., Kim, J.W., Kislov, A., Kitoh, A., Loutre, M.F., Masson, V., McAvaney, B., McFarlane, N., de Noblet, N., Peltier, W.R., Peterschmitt, J. Y., Pollard, D., Rind, D., Royer, J.F., Schlesinger, M.E., Syktus, J., Thompson, S., Valdes, P., Vettoretti, G., Webb, R.S., Wyputta, U., 1999. Monsoon changes for 6000 years ago: results of 18 simulations from the Paleoclimate Modeling Intercomparison Project (PMIP). Geophysical Research Letters 26 (7), 859–862.

Kalnay, E., Kanamitsu, M., Kistler, R., Collins, W., Deaven, D., Gandin, L., Iredell, M., Saha, S., White, G., Woollen, J., Zhu, Y., Chelliah, M., Ebisuzaki, W., Higgins, W., Janowiak, J., Mo, K.C., Ropelewski, C., Wang, J., Leetmaa, A., Reynolds, R., Jenne, R., Joseph, D., 1996. The NCEP/NCAR 40-year reanalysis project. Bulletin of the American Meteorological Society 77 (3), 437–471.

Kaufman, D.S., Porter, S.C., Gillespie, A.R., 2004. Quaternary alpine glaciation in Alaska, the Pacific Northwest, Sierra Nevada, and Hawaii, in Gillespie A.R., Porter S.C., and Atwater B.F., eds., The Quaternary Period in the United States. Developments in Quaternary Science Vol. 1, Elsevier Press, 77–103.

Kayastha, R.B., Ohata, T., Ageta, Y., 1999. Application of a mass-balance model to a Himalayan glacier. Journal of Glaciology 45 (151), 559–567.

Kuhle, M., 1998. Reconstruction of the 2.3 million km^2 late Pleistocene ice sheet on the Tibetan Plateau and its impact on the global climate. Quaternary International 47 (8), 173–182.

Kutzbach, J.E., Gallimore, R.G., 1988. Sensitivity of a coupled atmosphere/mixed layer ocean model to changes in orbital forcing at 9000 years B.P. Journal of Geophyscial Research 93 (D1), 803–821.

Legates, D.R., Willmott, C.J., 1990a. Mean seasonal and spatial variability in gauge-corrected, global precipitation. International Journal of Climatology 10 (2), 111–127.

Legates, D.R., Willmott, C.J., 1990b. Mean seasonal and spatial variability in global surface air-temperature. Theoretical and Applied Climatology 41 (1–2), 11–21.

Lowell, T.V., Heusser, C.J., Andersen, B.G., Moreno, P.I., Hauser, A., Heusser, L.E., Schluchter, C., Marchant, D.R., Denton, G.H., 1995. Interhemispheric correlation of late Pleistocene glacial events. Science 269 (5230), 1541–1549.

Mantua, N.J., Hare, S.R., Zhang, J., Wallace, J.M., Francis, R.C., 1997. A Pacific decadal climate oscillation with impacts on salmon. Bulletin of the American Meteorological Society 78, 1069–1079.

Molg, T., Hardy, D.R., 2004. Ablation and associated energy balance of a horizontal glacier surface on Kilimanjaro. Journal of Geophysical Research 109 (D16) Art. No. D16104.

Owen, L.A., Benn, D.I., 2005. Equilibrium-line altitudes of the Last Glacial Maximum for the Himalaya and Tibet: an assessment and evaluation of results. Quaternary International 138, 55–78.

Owen, L.A., Kamp, U., Spencer, J.Q., Haserodt, K., 2002. Timing and style of Late Quaternary glaciation in the eastern Hindu Kush, Chitral, northern Pakistan: a review and revision of the glacial chronology based on new optically stimulated luminescence dating. Quaternary International 97 (8), 41–55.

Owen, L.A., Finkel, R.C., Haizhou, M., Spencer, J.Q., Derbyshire, E., Barnard, P.L., Caffee, M. W., 2003. Timing and style of Late Quaternary glaciation in northeastern Tibet. Geological Society of America Bulletin 115 (11), 1356–1364.

Owen, L.A., Finkel, R.C., Barnard, P.L., Haizhou, M., Asahi, K., Caffee, M.W., Derbyshire, E., 2005. Climatic and topographic controls on the style and timing of Late Quaternary glaciation throughout Tibet and the Himalaya defined by 10Be cosmogenic radionuclide surface exposure dating. Quaternary Science Reviews 24 (12–13), 1391–1411.

Owen, L.A., Caffee, M., Finkel, R., Seong, Y., 2008. Quaternary glaciation of the Himalayan-Tibetan orogen. Journal of Quaternary Science 23 (6–7), 513–531.
Paterson, 1999. Physics of Glaciers. Pergamon/Elsevier Science Inc.
Phillips, W.M., Sloan, V.F., Shroder, J.F., Sharma, P., Clarke, M.L., Rendell, H.M., 2000. Asynchronous glaciation at Nanga Parbat, northwestern Himalaya Mountains. Pakistan. Geology 28 (5), 431–434.
Porter, S.C., 1975. Equilibrium-line altitudes of late Quaternary glaciers in southern Alps, New Zealand. Quaternary Research 5 (1), 27–47.
Porter, S.C., 1977. Present and past glaciation threshold in the Cascade Range, Washington, U. S. A.: topographic and climatic controls, and paleoclimatic implications. Journal of Glaciology 18, 101–116.
Porter, S.C., Orombelli, G., 1985. Glacier contraction during the middle Holocene in the western Italian Alps — evidence and implications. Geology 13 (4), 296–298.
Ramanathan, Y., 1987. Cumulus parameterization in a case-study of a monsoon depression. Monthly Weather Review 108 (3), 313–321.
Richards, B., Benn, D.I., Owen, L.A., Rhodes, E.J., Spencer, J.Q., 2000. Timing of late Quaternary glaciations south of Mount Everest in the Khumbu Himal, Nepal. Geological Society of America Bulletin 112, 1621–1632.
Rupper, S.B., Roe, G.H., 2008. Glacier changes and regional climate: a mass and energy balance approach. Journal of Climate 21 (20), 5384–5401.
Schafer, J.M., Tschudi, S., Zhao, Z.Z., Wu, X.H., Ivy-Ochs, S., Wieler, R., Baur, H., Kubik, P. W., Schluchter, C., 2002. The limited influence of glaciations in Tibet on global climate over the past 170 000 yr. Earth and Planetary Science Letters 194 (3–4), 287–297.
Seong, Y.B., Owen, L.A., Bishop, M.P, Bush, A., Clendon, P., Copland, L., Finkel, R., Kamp, U., Shroder, J.F., 2007. Quaternary glacial history of the central Karakoram. Quaternary Science Reviews 26 (25–28), 3384–3405.
Sharma, M.C., Owen, L.A., 1996. Quaternary glacial history of NW Garhwal, Central Himalayas. Quaternary Science Reviews 15, 335–365.
Shi, Y., 2002. Characteristics of late Quaternary monsoonal glaciation on the Tibetan Plateau and in East Asia. Quaternary International 97 (8), 79–91.
Trenberth, K., 1997. The definition of El Niño. Bulletin of the American Meteorological Society 78, 2771–2777.
Tschudi, S., Schäfer, J.M., Zhao, Z., Wu, X., Ivy-Ochs, S., Kubik, P.W., Schlüchter, C., 2003. Glacial advances in Tibet during the Younger Dryas? Evidence from cosmogenic ^{10}Be, ^{26}Al, and ^{21}Ne. Journal of Asian Earth Sciences 22, 301–306.
Vettoretti, G., Peltier, W.R., McFarlane, N.A., 1998. Simulations of mid-Holocene climate using an atmospheric general circulation model. Journal of Climate 11 (10), 2607–2627.
Wallace, J.M., Gutzler, D.S., 1981. Teleconnections in the geopotential height field during the Northern Hemisphere Winter. Monthly Weather Review 109, 784–812.
Wallace, J., Hobbs, W., 2005. Atmospheric Science: an Introductory Survey. Academic Press.
Wang, Y., Zhu, 2005. Studies of chronology of millennial time scale climate oscillations in the Holocene. Advances in Climate Change Research 1 (4), 157–160.
Wang, Y., Cheng, H., Edwards, R.L., He, Y., Kong, X., An, Z., Wu, J., Kelly, M.J., Dykoski, C.A., Li, X., 2005. The Holocene Asian monsoon: links to solar changes and north Atlantic climate. Science 308 (5273), 854–857.
Wei, Z., Zhijiu, C., Yanghua, L., 2006. Review of the timing and extent of glaciers during the last glacial cycle in the bordering mountains of Tibet and in East Asia. Quaternary International 154 (155), 32–43.
Wilcox, E.M., Ramanathan, V., 2001. Scale dependence of the thermodynamic forcing of tropical monsoon clouds: results from TRMM observations. Journal of Climate 14 (7), 1511–1524.
Xiang, R., Sun, Y.B., Li, T.G., Oppo, D.W., Chen, M.H., Zheng, F., 2007. Paleoenvironmental change in the middle Okinawa Trough since the last deglaciation: evidence from the sedimentation rate and planktonic foraminiferal record. Palaeogreography, Palaeoclimatology, Palaeoecology 243 (3–4), 378–393.
Yang, B., Bräuning, A., Dong, Z., Zhang, Z., Keqing, J., 2008. Late Holocene monsoonal temperate glacier fluctuations on the Tibetan Plateau. Global and Planetary Change 60 (1–2), 126–140.
Zhang, Y., Shiyin, L., Yongjian, D., 2006. Observed degree-day factors and their spatial variation on glaciers in western China. Annals of Glaciology 43, 301–306.
Zhou, S.Z., Xu, L.B., Colgan, P.M., Michelson, D.M., Wang, X.L., Wang, J., Zhong, W., 2007. Cosmogenic Be-10 dating of Guxiang and Baiyu glaciations. Chinese Science Bulletin 52 (10), 1387–1393.